J Mater Sci (2009) 44:1851–1857
DOI 10.1007/s10853-008-3240-7

Electrophoretic deposition of ZrO_2–Y_2O_3: a bi-component study concerning self-assemblies

Ricardo H. R. Castro · Paulo K. Kodama · Douglas Gouvêa · R. Muccillo

Received: 12 May 2008 / Accepted: 31 December 2008 / Published online: 3 February 2009

Abstract There are many industrial advantages of using mechanical multi-oxides mixtures to obtain ceramic parts by electrophoretic deposition (EPD). This is mainly because one could avoid complex chemical synthesis routes to achieve a desirable composition. However, EPD of these suspensions is not an easy task as well since many different surfaces are present, leading to unexpected suspension behavior. The particles surface potentials and interactions can, however, be predicted by an extension of the DLVO theory. Using this theory, one can control the suspension properties and particles distribution. The objective of this work was to apply the colloidal chemistry theories to promote the formation of a heterocoagulation between ZrO_2 and Y_2O_3 particles in ethanol suspension to achieve a suitable condition for EPD. After identifying a condition where those particles had opposite surface charges and adequate relative sizes, heterocoagulation was observed at operational pH 7.5, generating an organized agglomerate with ZrO_2 particles surrounding Y_2O_3, with a net zeta potential of −16.6 mV. Since the agglomerates were stable, EPD could be carried out and homogeneous deposits were obtained. The deposited bodies were sintered at 1600 °C for 4 h and partially stabilized ZrO_2 could be obtained without traces of Y_2O_3 second phases.

R. H. R. Castro (✉) · P. K. Kodama
CDMat – Department of Materials Engineering, FEI University Center, Av. Humberto A.C. Branco, 3972, São Bernardo do Campo, SP 09850-901, Brazil
e-mail: rhrcastro@fei.edu.br

D. Gouvêa
Department of Metallurgical and Materials Engineering, Escola Politécnica, University of São Paulo, Av. Prof. Mello Moraes, 2463, São Paulo, SP 05508-900, Brazil

R. Muccillo
Centro Multidisciplinar para o Desenvolvimento de Materiais Cerâmicos – CCTM – Instituto de Pesquisas Energéticas e Nucleares, C. P. 11049, Pinheiros, São Paulo, SP 05422-970, Brazil

Introduction

The electrophoretic deposition (EPD) of multi-component systems has been described to be a complex and tricky task [1]. This is because one can expect that when differently charged particles are in suspension, the particles with positive surface potential will deposit on the cathode, while those with negative surface potential will deposit on the anode. However, this simplistic approach neglects the interactions between the particles that can be predicted by an extension of the DLVO theory. This extension was reported previously [2–4] describing a general relation expressing the interaction between the electrical double layers surrounding any two similar or dissimilar particles. The potential of interaction between particles of different radii and with different surface potential can be expressed by V_R:

$$V_R = \frac{\pi\varepsilon_o\varepsilon_r a_1 a_2(\psi_1^2+\psi_2^2)}{(a_1+a_2)} \times \left\{ \frac{2\psi_1\psi_2}{(\psi_1^2+\psi_2^2)} \ln\left[\frac{1+\exp(-\kappa H)}{1-\exp(-\kappa H)}\right] + \ln\left[1-\exp(-2\kappa H)\right] \right\} \quad (1)$$

where κ is the Debye parameter [4], H is the distance between the particles, ε_o is the dielectric permittivity of

vacuum, ε_r is the relative dielectric constant of the solvent, a_1, a_2 and ψ_1, ψ_2 are the radii and surface potentials of two dissimilar particles, respectively. V_R will act in addition to the van der Waals potential for the two interacting particles, which can be expressed by [4]:

$$V_A = -\frac{A_{132}}{12}\left[\frac{y}{x^2+xy+x}+\frac{y}{x^2+xy+x+y} + 2\ln\left(\frac{x^2+xy+x}{x^2+xy+x+y}\right)\right] \quad (2)$$

where $x = H/(a_1+a_2)$, $y = a_1/a_2$, and $A_{132} \approx (A_{11}^{1/2} - A_{33}^{1/2})\cdot(A_{22}^{1/2} - A_{33}^{1/2})$. A_{11} and A_{22} are the Hamaker constants for particles 1 and 2 in vacuum, and A_{33} is the Hamaker constant of the solvent.

The total potential, defined as $V_T = V_R + V_A$, predicts that opposite charged particles will heterocoagulate in suspension, i.e., the particles will agglomerate since the total potential between them will be of attraction. A number of works published have been dedicated to the description of this phenomenon for different materials [3–7], providing information of how to control it by using variables such as the Hamaker constant, the surface potentials, the ionic concentration of the medium, the relative sizes of the particles, and the characteristics of the solvent (as pointed in the equations above). However, only a few works have explored this phenomenon as a promising tool in the EPD process [7, 8]. This is because low net surface charge could be expected on the surface of the agglomerates due to the particles charge compensation. Nevertheless, a relatively high net charge can be achieved by controlling the above-mentioned surface potentials and particle sizes, as will be shown in this work for the technologically important ZrO_2–Y_2O_3 system with a detailed discussion based on an extension of the DLVO theory.

ZrO_2–Y_2O_3 is an important material for fuel cells technologies [9, 10]. In these devices, the needed thin films of yttrium-stabilized zirconia (YSZ) can be applied by different techniques, including EPD [11]. The literature regarding EPD of YSZ reports the usage of powders or nanopowders synthesized by chemical routes or commercial powders [9, 10, 12, 13]. In any of these cases, a single particle type is in suspension. However, one cannot neglect the important economical benefits of the usage of a direct mixture of ZrO_2 and Y_2O_3 particles in the suspension. This mixture, however, will be subjected to interacting potentials among the particles, V_R and V_A. In the present work, we explore the particles interactions in a mechanical mixture of ZrO_2 with 8 mol% Y_2O_3 in ethanol to promote controlled agglomerates with a remaining zeta (ζ)-potential to submit the system to EPD. Particle size was verified to be an important variable to obtain the desired heteroagglomerate characteristics.

Experimental procedure

Electrophoretic mobility measurements were used to calculate the ζ-potential and were performed in suspensions prepared to a solid loading of 1 vol% using ESA-9800 equipment (Matec Applied Sciences, USA), which measures simultaneously pH, electrophoretic mobility, ionic conductivity, and temperature. The suspensions were prepared using ZrO_2 (99.9%, Sigma-Aldrich) and Y_2O_3 (99.9%, Sigma-Aldrich). Solvent was ethanol (purity higher than 99.5%, Synth; H_2O content <0.2%; methanol content <0.1%). ZrO_2 containing 8 mol% Y_2O_3, hereafter called Z8Y, was prepared by mechanical mixing of the components. All suspensions were ball-milled using zirconia milling balls for 4 h before the analysis. The pH adjustments were carried out using HNO_3 and NaOH (analytical grade, Synth) in 2 M ethanol solutions. All measurements were carried out at 25 °C.

The pH measurements in the ethanol suspensions were carried out using a common pH meter, providing the so-called "operational pH". The acidity of a nonaqueous system can be estimated using the equation at 25 °C [4, 14]:

$$pa_H = pH - \frac{\Delta E_j}{0.05916} \quad (3)$$

where ΔE_j is the difference between the liquid-junction potentials from the standard solution and the testing one. For an aqueous KCl buffer solution, and ethanol testing solution, ΔE_j was estimated to be about −0.073 [4, 14].

Viscosimetry studies were also carried out using Brookfield DV-II equipment at 25 °C using spindle no. 18. In this case, the suspensions were prepared to a solid loading of 5 vol% to increase signal reliability.

The particles morphology and spatial distribution in the suspensions were analyzed by scanning electron microscopy (SEM) using LEO Stereoscan 440 with high vacuum (2.5×10^{-6} Torr), secondary electron detectors for images (10.00 kV), and scattered electrons for energy dispersive spectroscopy (EDS) (12.00 kV, Ge detector and INCA v.16 Software, Oxford). The SEM samples were prepared by dropping dilute ethanol suspensions on Al substrates, drying at 70 °C for 4 h, and applying pure conductive Au coating. SEM of a sintered deposit was also carried out in the same condition after application of the Au coating.

The particle size distributions were obtained by laser diffraction/scattering using a Mastersizer S (Malvern Instruments) in alcohol. During measurement, the particle dispersion was stirred at 2500 rpm and samples were ultrasonicated for 1 min before particle size measurements. The average particle sizes D [3, 4] of the as-received particles were 0.49 and 2.92 μm for ZrO_2 and Y_2O_3, respectively. Another set of ZrO_2 particle size was created

by calcination at 1200 °C for 5 h. The average size of the new ZrO_2 was 1.91 μm.

Electrophoretic deposition was carried out using an equipment specially designed to fulfill the experimental needs. It has a cylindrical geometry, with a 2-mm-diameter graphite electrode placed in the middle of a cylindrical stainless steel counter electrode with diameter of 22 mm. The distance between the deposition graphite electrode surface and the counter electrode was 10 mm. The deposition chamber was placed over an analytical balance to measure the deposited mass as a function of time and applied voltage using suspension containing 5 vol% of solid loading. The applied voltages were within the 30–150 V range.

Sintering studies were carried out in the deposited body after EPD using 150 V in a SETSYS 1600 TMA Setaram equipment, France. The sample was heated up to 1600 °C at 10 °C/min, kept at that temperature for 4 h, and finally cooled at 30 °C/min. All experiments were conducted under synthetic air flux at 20 mL/min. X-ray diffraction was carried out in the sintered sample with a model D8 Advance Bruker AXS diffractometer, Cu Kα radiation ($\lambda = 1.5406$ Å), to identify the obtained phases after sintering.

Results and discussion

Figure 1 shows the ζ-potential measurements for both pure ZrO_2 and pure Y_2O_3 suspensions in ethanol. The isoelectric points (IEP) for ZrO_2 and Y_2O_3 were determined to be 4.6 and 9.6 ($pa_H = 5.83$ and 10.83), respectively, being consistent with the literature data [15]. The ζ-potential curves are consistent with common oxides suspensions, with negative potentials when the pH is above the IEP, and a positive potential at pH below IEP. At operational pH 7.5 ($pa_H = 8.73$), the graph indicates that ZrO_2 and Y_2O_3 surfaces have opposite electrical charges. ZrO_2 particles are negatively charged with ζ-potential of about −30 mV, while at the same pH, Y_2O_3 particles are positively charged with ζ-potential of about +23 mV. The presented ζ-potential data are consistent with the viscosity measurements presented in Fig. 2 as a function of pH at 200 rpm. For pH close to the IEP, both samples show high viscosity due to natural agglomeration. At operational pH around 7.5, both suspensions have low viscosity as a result of the breakage of agglomerates due to the relatively high ζ-potential.

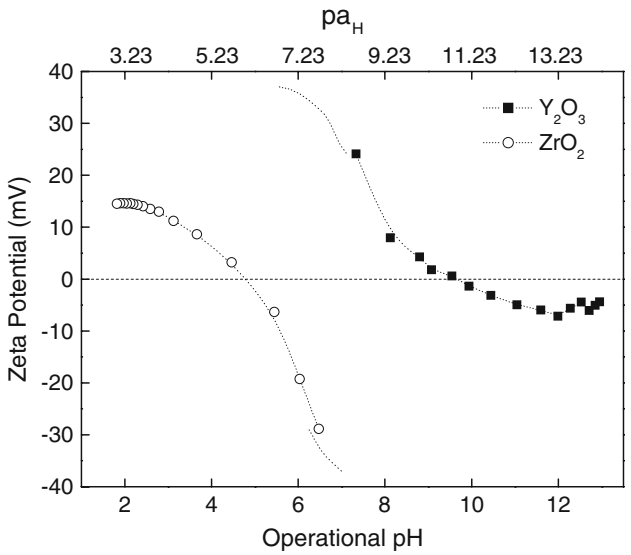

Fig. 1 Zeta potential as a function of operational pH (and pa_H) for pure ZrO_2 ethanol suspension and pure Y_2O_3 ethanol suspension showing that at operational pH 7.5 the ZrO_2 and Y_2O_3 have opposite charges

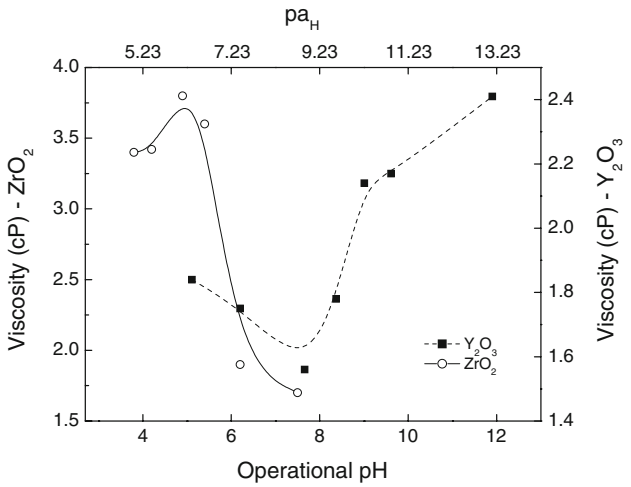

Fig. 2 Viscosity as a function of operational pH (and pa_H) for pure ZrO_2 or pure Y_2O_3 ethanol suspensions. Higher viscosities are observed near the isoelectric points for both samples as expected by ζ-potential measurements

The observed ζ-potentials at operational pH 7.5 are suitable for promoting the heterocoagulation between zirconia and yttria driven by electrostatic interactions [8]. Since the potential for heterocoagulation also depends on the particles radii, two sets of particles were studied in this work. The average particle sizes D [3, 4] were 0.49 and 1.91 μm for ZrO_2, and 2.92 μm for Y_2O_3, measured by laser scattering technique.

The interacting potentials between ZrO_2 (with radius 0.49 and 1.91 μm) and Y_2O_3 particles as a function of the distance between them, calculated using Eqs. 1 and 2, are shown in Fig. 3. The total potentials are of attraction in both cases, indicating a clear condition for heterocoagulation. However, the potential of attraction between the ZrO_2 and Y_2O_3 is stronger for the larger ZrO_2 particles. This indicates stronger agglomerates, in principle more indicated for electrophoresis purposes.

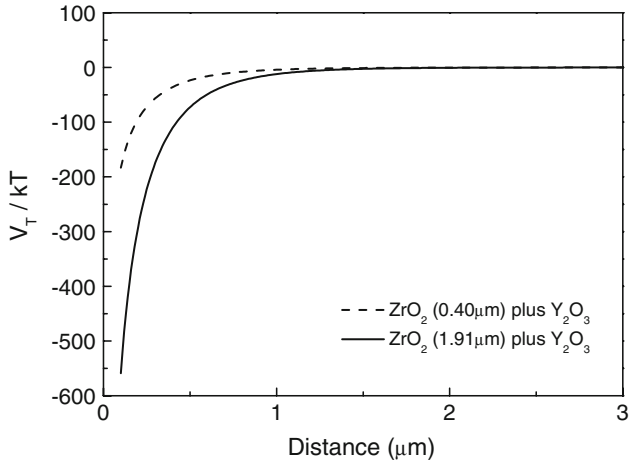

Fig. 3 Total interaction potential between Y_2O_3 and ZrO_2 with 1.91 μm (*solid line*); and between Y_2O_3 and ZrO_2 with 0.40 μm (*dashed line*) in ethanol suspension at operational pH 7.5 ($\kappa = 3.2 \times 10^6\ m^{-1}$; $A_{11}[Y_2O_3] = 13.3 \times 10^{-20}$ J; $A_{11}[ZrO_2] = 20.3 \times 10^{-20}$ J; $A_{33}[\text{ethanol}] = 4.2 \times 10^{-20}$ J)

To confirm the presence of agglomerates resulting from heterocoagulation, SEM of the dried powder from a mechanically mixed mixture Z8Y suspension in ethanol at operational pH 7.5 was carried out. Figure 4c shows the micrograph of the organized agglomerate with ZrO_2 particles surrounding Y_2O_3 as identified by both morphology (comparing to isolated particles in Fig. 4a, b) and EDS measurements and indicated in the figure.

The mobility of the formed agglomerate can be predicted by an evaluation of the surface potential simulation using an extension of the DLVO theory. Figure 5 shows the interacting potential from the free surface of Y_2O_3 particle (solid line) simulated using regular equations for the repulsive energy and van der Waals energy of attraction for spheres of similar radii [4, 16], and using data provided by ESA-9800 measurements (ionic concentration and valence, potential, and temperature). The presence of a ZrO_2 particle near Y_2O_3 surface due to the heterocoagulation will affect its potential. However, this interaction will depend on the relative position of the particle, which directly depends on its size. For instance, Fig. 5 shows the potential of a ZrO_2 particle with 0.4 μm (dotted line) at a short distance from the surface of Y_2O_3 (<0.1 μm). Since the ZrO_2 potential is of opposite charge to the Y_2O_3 potential, this will cause interactions between both diffuse layers, and the total potential can be estimated by the sum of the potentials. Since for 0.4 μm ZrO_2 the modulus of the potential is slightly smaller than that of the Y_2O_3 surface, a slight positive potential for the agglomerate is expected (Fig. 6). This will not occur for larger ZrO_2 particles, as shown by Fig. 5 (dashed line). In this case, the ZrO_2 potential does not overlap the region of the Y_2O_3 electrical double layer with higher potential modulus, and hence, the total potential is expected to be negative and with higher modulus for this agglomerate (Fig. 6). The total potential in Fig. 6, resulted from the sum of ZrO_2 and Y_2O_3 taking into account the relative positions, can be fitted by the DLVO theory and provides a ζ-potential of −16.6 mV for the 1.91 μm $ZrO_2 + Y_2O_3$ agglomerate and +4.2 mV for the 0.4 μm $ZrO_2 + Y_2O_3$ agglomerate.

Thereafter, one may expect that the assembled structure 1.91 μm $ZrO_2 + Y_2O_3$ could be moved by

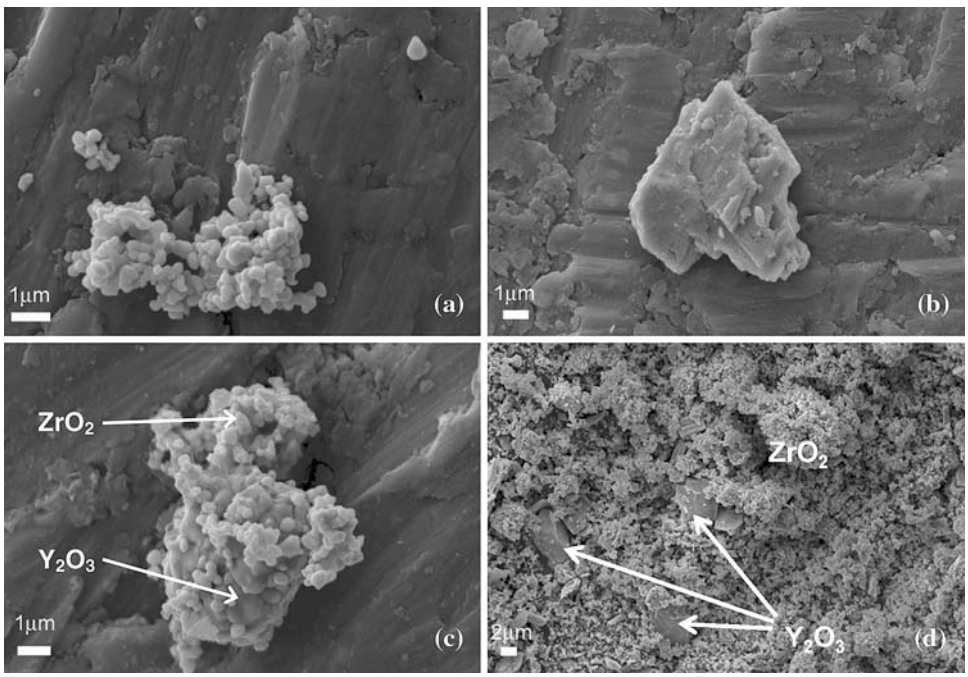

Fig. 4 SEM of particles dried from ethanol suspensions at operational pH 7.5. **a** ZrO_2 isolated particle. **b** Y_2O_3 isolated particle. **c** Organized agglomerate (from heterocoagulation) showing ZrO_2 particle surrounding Y_2O_3 (identity of the particles identified by both morphology comparison and EDS). **d** Micrograph of the deposit after EPD of a ZrO_2–8 mol% Y_2O_3 mechanical mixture showing Y_2O_3 surrounded by ZrO_2 particles in the deposit

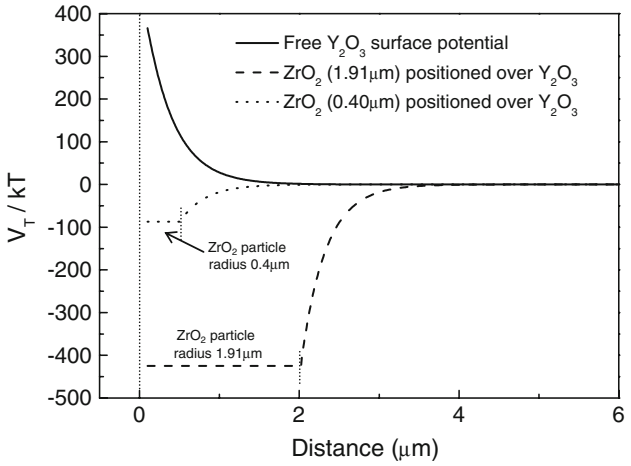

Fig. 5 Total interaction potential of free Y_2O_3 (*solid line*), ZrO_2 particle with 1.91 μm attached to Y_2O_3 (*dashed line*), and ZrO_2 particle with 0.40 μm attached to Y_2O_3 (*dotted line*). The *horizontal lines* with constant potentials (indicated as "ZrO_2 particle radius") represent the space occupied by the ZrO_2 particles from the attaching surface. All potentials in ethanol suspensions are at operational pH 7.5

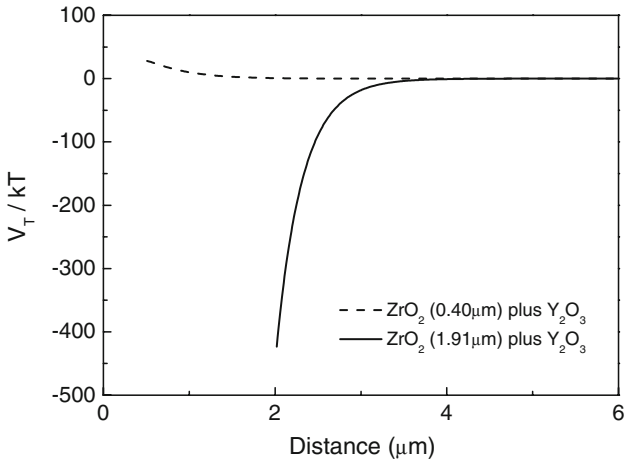

Fig. 6 Total interaction potential between agglomerates of Y_2O_3–ZrO_2 for the two sizes of zirconia particles (0.4 and 1.91 μm) in ethanol suspension at operational pH 7.5

electrophoresis without breakage due to the strong attractions between particles and the relatively high net charge. Figure 7 shows the deposited mass as a function of time for EPD process in a mechanical mixture of ZrO_2 (1.91 μm) and 8 mol% of Y_2O_3 suspension at operational pH 7.5 at different applied voltages. One may observe a mostly linear evolution of the deposited mass with increasing deposition time for all applied voltages. Moreover, the slope of the curves increases as the applied voltage increases; suggesting that the particles are moving faster as the voltage increases. The linear behavior in all conditions indicates that the organized agglomerates do not break upon electrophoresis in any condition (even for the higher voltages),

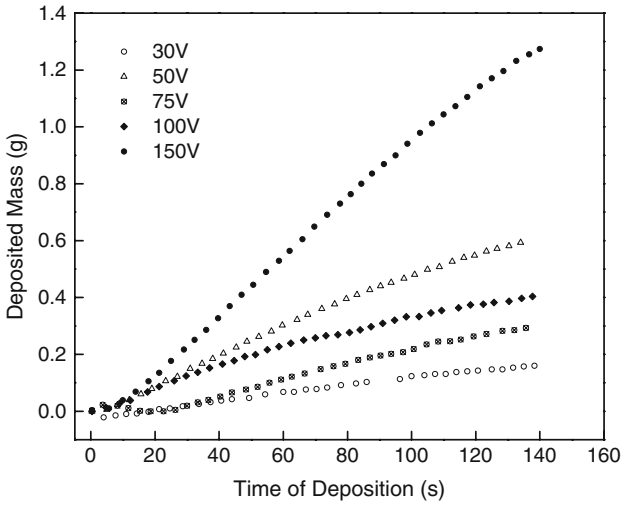

Fig. 7 Deposited mass during EPD of ZrO_2–8 mol% Y_2O_3 mechanical mixtures as a function of time and applied voltage

and a homogeneous deposit could be therefore expected. Breakage of the agglomerates would change the average speed of deposition, changing the linear slope.

To observe the quality of the green as-deposited body in terms of particles distribution, SEM of the obtained deposit is shown in Fig. 4d for the sample submitted to EPD at 150 V. Note that both ZrO_2 and Y_2O_3 particles are observed in the deposit. The arrows in the figure show the Y_2O_3 particles surrounded by the ZrO_2 ones, indicating that the agglomerate is maintained during EPD and after deposition. The attained homogeneity of the deposit can also be evaluated after sintering of the body. Figure 8 shows the dilatometry of the deposit obtained at 150 V EPD. The sample was sintered up to 1600 °C with a 4 h isotherm. Upon heating, the sample showed nonsignificant changes up to 1000 °C. At this point, the sample suffered abrupt expansions probably due to phase transformation from monoclinic to cubic and solid solution of Y_2O_3 in ZrO_2. After that, the sample started to shrink due to sintering, and a total shrinkage of 16.5% could be observed. During cooling of the sample, the shrinkage is linear with T, indicating that the phase transition from cubic to monoclinic is not present due to stabilization by Y_2O_3. Figure 9 shows the XRD pattern of the sample after sintering. Traces of Y_2O_3 could not be observed (evidenced by the peaks at $2\theta = 20.45$, 29.16, and 33.78°—JCPDS 05-0574), reflecting total solution of this phase in the ZrO_2 structure. The observed reflections at $2\theta = 30$, 34.8, and 73.7° assure that the structure of the sintered specimen is cubic fluorite. Traces of monoclinic could be detected (28.2°) by the XRD pattern. This indicates that, despite Y_2O_3 particles are homogeneously distributed throughout the deposited body promoting ZrO_2 stabilization, the amount was not enough to promote full stabilization (as

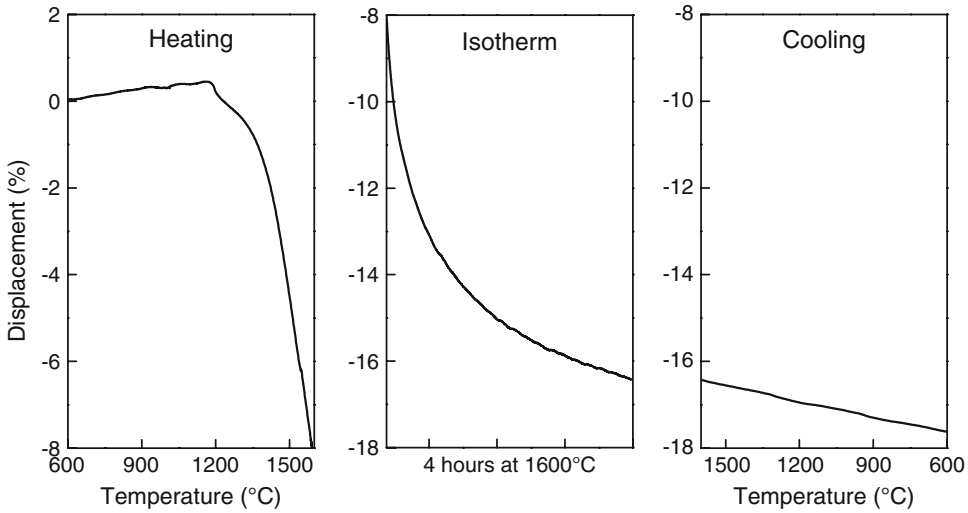

Fig. 8 Dilatometry measurements in the deposit obtained by EPD at 150 V. The first part shows the heating at 10 °C/min up to 1600 °C. The second stage shows the displacement during an isotherm at 1600 °C for 4 h. The last part shows the cooling at 30 °C/min

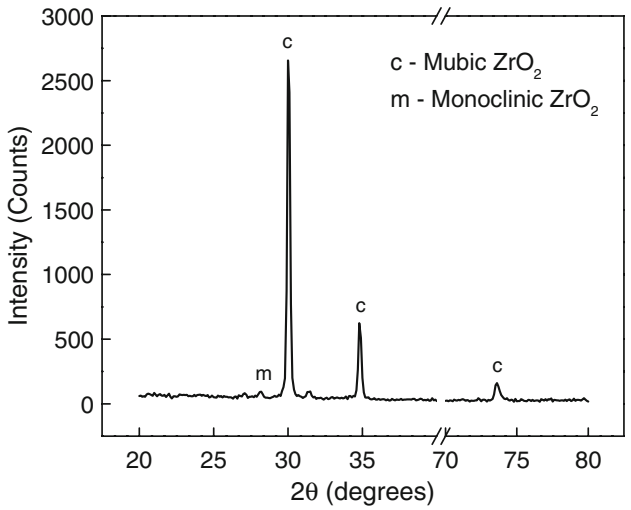

Fig. 9 XRD pattern of the deposited body obtained by EPD at 150 V and sintered at 1600 °C for 4 h. Cubic ZrO_2 (*c*) and traces of monoclinic ZrO_2 (*m*) could be detected

expected by the concentration), leading to the small amount of monoclinic phase at room temperature, which could not be detected by the dilatometry studies. SEM of the sintered body is shown in Fig. 10. The figure shows high homogeneity of the sintered bodies, however, with relatively high porosity. This is probably related to the large initial particle sizes that decreased the driving force for sintering. However, there is no reason to believe that the promoted heretocoagulation and subsequent EPD are restricted to micropowders, and future works on nanosized particles will enable high density of the deposited body.

Conclusion

Using the theory of heterocoagulation, organized agglomerate was induced in an ethanol suspension containing Y_2O_3 and ZrO_2 particles. The agglomerate was observed by SEM, showing ZrO_2 particles surrounding Y_2O_3. The interacting potentials between these particles were calculated and electrical double layer of the agglomerate was estimated by superposing the potentials from both particles.

The ζ-potential for the agglomerate was shown to be highly dependent on the radius of the ZrO_2 particle, since this determines the superposition of the potentials. Using ZrO_2 particles of 1.91 μm and Y_2O_3 particles of 2.92 μm,

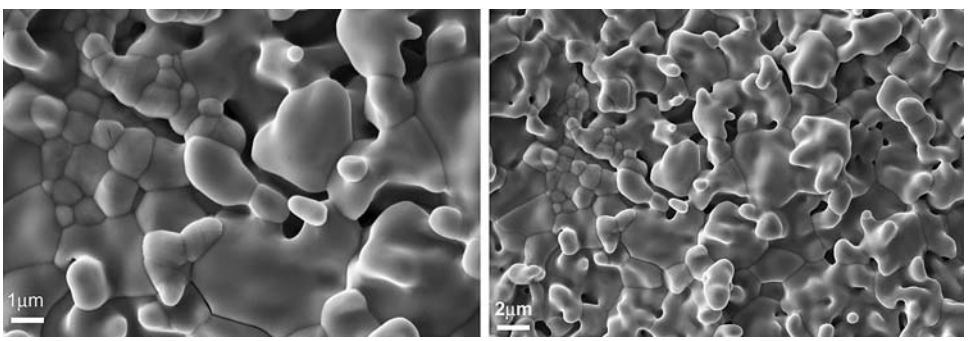

Fig. 10 SEM of the deposited body obtained by EPD at 150 V and sintered at 1600 °C for 4 h

agglomerate with −16.6 mV of ζ-potential was obtained. This agglomerate was strong enough not to be broken down during the EPD process, and homogeneous bodies were obtained at different voltages. The deposited body did not show cracks and could be sintered at 1600 °C to promote the formation of Y_2O_3 solid solution in the ZrO_2 structure. Both dilatometry and XRD data showed that, as expected, the obtained zirconia after sintering was partially stabilized and without traces of Y_2O_3 second phases.

Acknowledgements The authors wish to thank FAPESP (Fundação de Amparo à Pesquisa do Estado de São Paulo) Procs. 05/53241-9 and 05/55335-0, and CAPES (Coordenação do Aperfeiçoamento de Pessoal de Nível Superior) for the financial support.

References

1. Besra L, Liu M (2007) Prog Mater Sci 52:1
2. Hogg R, Healy TW, Fuerstenau DW (1966) Trans Faraday Soc 62:1638
3. Derjaguin BV (1954) Discuss Faraday Soc 18:60
4. Wang G, Nicholson PS (2001) J Am Ceram Soc 84:1250
5. Bleier A, Westmoreland G (1991) J Am Ceram Soc 74:3100
6. Mitchell TK, Nguyen AV, Evans GM (2005) Adv Colloid Interface Sci 114–115:227
7. Boccaccini AR, Trusty PA, Tanplin DMR, Ponton CB (1996) J Eur Ceram Soc 16:1319
8. Castro RHR, Marcos PJB, Gouvea D (2007) J Mater Sci 42:6946. doi:10.1007/s10853-006-1279-x
9. Jia L, Lu Z, Huang X, Liu Zy, Chen K, Sha X, Li G, Su W (2006) J Alloys Compd 424:299
10. Negishi H, Yamaji K, Sakai N, Horita T, Yanagishita H, Yokokawa H (2004) J Mater Sci 39:833. doi:10.1023/B:JMSC.0000012911.86185.13
11. Boccaccini AR, Zhitomirsky I (2002) Curr Opin Solid State Mater Sci 6:251
12. Negishi H, Yamaji K, Imura T, Kitamoto D, Ikegami T, Yanagishita H (2005) J Electrochem Soc 152:J16
13. Chen FL, Liu ML (2001) J Eur Ceram Soc 21:127
14. Wang G, Sarkar P, Nicholson PS (1997) J Am Ceram Soc 80:965
15. Bohmer MR, Heesterbeek WHA, Deratani A, Renard E (1995) Colloids Surf A 99:53
16. Cao G (2004) Nanostructures and nanomaterials: synthesis, properties, and applications. Imperial College Press, Danvers